Stepped spillway flows and air entrainment

HUBERT CHANSON
Department of Civil Engineering, The University of Queensland, St. Lucia, QLD 4072, Australia

Received April 2, 1992
Revised manuscript accepted August 7, 1992

Stepped spillways have become a popular method for handling flood releases. The steps significantly increase the rate of energy dissipation taking place on the spillway face and reduce the size of the required downstream energy dissipation basin. The compatibility of stepped spillways with roller compacted concrete and gabion construction techniques results in low additional cost for the spillway. This paper presents a review of recent developments for the design of stepped spillways, provides a discussion of the effects of air entrainment, and presents new calculation methods that take into account the effects of flow aeration on the flow characteristics and the rate of energy dissipation.

Key words: stepped spillway, air entrainment, dam, spillway, energy dissipation.

Les évacuateurs de crues en marches d'escalier sont devenus une méthode courante pour décharger les crues. Les seuils des marches augmentent considérablement la dissipation d'énergie au long du déservoir, et, de ce fait, réduisent la taille du bassin de dissipation en aval de l'évacuateur de crues. La géométrie des déservoirs en marches d'escalier s'adapte très bien à des structures en gabions ou en béton compacté au rouleau, et n'entraîne qu'une augmentation raisonnable du coût de construction. Le présent article décrit de récents développements dans le dimensionnement de ce type de déversoir. Puis l'auteur discute les effets de l'entraînement d'air, et il présente une nouvelle méthode de calculs pour des écoulements aérés au dessus des évacuateurs de crues en marches d'escalier.

Mots clés : évacuateurs de crues en marches d'escalier, entraînement d'air, barrage, déversoirs, dissipation d'énergie.

Can. J. Civ. Eng. **20**, 422–435 (1993)

Introduction

Presentation

Energy dissipation over dam spillways is usually achieved by (*i*) a standard stilling basin downstream of the spillway where a hydraulic jump is created to dissipate a large amount of flow energy, (*ii*) a high velocity water jet taking off from a flip bucket and impinging into a downstream plunge pool, or (*iii*) the construction of steps on the spillway to assist in energy dissipation.

Water flowing over a rough or stepped face of a dam can dissipate a major proportion of its energy. The steps significantly increase the rate of energy dissipation taking place on the spillway face, and eliminate or greatly reduce the need for a large energy dissipator at the toe of the spillway. Stepped spillways have become a popular method for flood releases at roller compacted concrete (RCC) dams and gabions dams. The compatibility of the stepped spillway design with RCC construction techniques results in low additional cost for the spillway (Frizell and Mefford 1991). Gabions are used frequently in the construction of small dams because the construction of gabion structures is easy and cheap. Gabion-stepped spillways are the most common type of spillway used for gabion dams (Stephenson 1979*a*; Degoutte *et al.* 1990).

So far, few analyses take into account the effects of air entrainment. In this paper the first part describes the flow characteristics and energy dissipation of non-aerated flows on a stepped spillway. In the second part, the effects of air entrainment on stepped spillway flows are discussed, and new formulations are proposed. The results are compared with recent experimental data (Table 1).

NOTE: Written discussion of this paper is welcomed and will be received by the Editor until October 31, 1993 (address inside front cover).

Printed in Canada / Imprimé au Canada

It must be noted that cavitation damage may occur on stepped spillways, but the risks of cavitation damage are reduced by the flow aeration. Peterka (1953) and Russell and Sheehan (1974) showed that 5–8% of air concentration next to the spillway bottom may prevent cavitation damage on concrete surfaces. Further, the high rate of energy dissipation along stepped spillways reduces the flow momentum. The reduction of flow velocity and the resulting increase of flow depth reduce the risks of cavitation as the cavitation index increases.

Step geometry

A stepped channel consists of an open channel with a series of drops along the invert. The total fall is divided into a number of smaller falls. Various step geometries are used: horizontal step, inclined step, and pooled step. This paper presents results that are applicable to stepped spillways with horizontal steps. The geometry of a horizontal step is defined by its height, h, and horizontal length, l, as shown in Figs. 1*b* and 1*c*. The step height and length are related to the spillway slope, α, by

$$[1] \qquad \tan \alpha = \frac{h}{l}$$

Essery and Horner (1978) and Peyras *et al.* (1991, 1992) discussed experimental results obtained with inclined steps. Vittal and Porey (1987) presented a cascade system of falls with pooled steps acting as intermediary energy dissipation basins.

Flow regimes above a stepped spillway

Two types of flow regime may occur above a stepped spillway: nappe flow and skimming flow (Fig. 1).

Peyras *et al.* (1991, 1992) indicated two types of nappe flow: (*i*) nappe flow with fully developed hydraulic jump

(Fig. 1*a*) for low discharge and small flow depth and (*ii*) nappe flow with partially developed hydraulic jump (Fig. 1*b*). The flow from each step hits the step below as a falling jet, with the energy dissipation occurring by jet breakup in air, by jet mixing on the step, and by the formation of a fully developed or partial hydraulic jump on the step (Rajaratnam 1990).

In the skimming flow regime, the water flows down the stepped face as a coherent stream, skimming over the steps and cushioned by the recirculating fluid trapped between them (Fig. 1*c*). Along the upstream steps, the flow is smooth and no air entrainment occurs. Downstream the flow is characterized by a large amount of flow aeration and strong vortices at the step toes (Fig. 2). Most of the energy is dissipated by momentum transfer between the main stream and the recirculating fluid.

For small dams and weirs, Ellis (1989) and Peyras *et al.* (1991, 1992) suggested that higher energy dissipation might occur in the nappe flow regime than in the skimming flow regime. However, nappe flow situations require relatively large steps, as detailed in the next paragraph. Such a geometry is not often practical but may apply to flat spillways, streams, and stepped channels.

Unaerated flow characteristics

Nappe flow

Flow parameters

Moore (1943) and Rand (1955) analyzed a single-step drop structure. Such a structure can be viewed as a single-step spillway. For a horizontal step, the flow conditions near the end of the step change from subcritical to critical at some section a short distance back from the edge. The flow depth at the brink of the step, d_b, is $d_b = 0.715 d_c$, where d_c is the critical flow depth (Rouse 1936). Application of the momentum equation to the base of the overfall leads to (White 1943)

$$[2] \quad \frac{d_1}{d_c} = 2^{1/2} \Big/ \left(\frac{3}{2^{3/2}} + \sqrt{\frac{3}{2} \frac{h}{d_c}} \right)$$

where d_1 is the flow depth at section 1 (Fig. 1*a*) and h is the step height. The total head, H_1, at section 1 can be expressed nondimensionally as

$$[3] \quad \frac{H_1}{d_c} = \frac{d_1}{d_c} + \frac{1}{2}\left(\frac{d_c}{d_1}\right)^2$$

The flow depth and the total head at section 2 (Fig. 1*a*) are given by the classical hydraulic jump equations:

$$[4] \quad \frac{d_2}{d_1} = \frac{1}{2}(\sqrt{1 + 8\mathrm{Fr}_1^2} - 1)$$

$$[5] \quad \frac{H_1 - H_2}{d_c} = \frac{(d_2 - d_1)^3}{4 d_1 d_2 d_c}$$

where Fr_1 is the Froude number defined at section 1: $\mathrm{Fr}_1 = q_w/\sqrt{g d_1^3}$. Rand (1955) assembled several sets of experimental data and developed the following correlations:

$$[6] \quad \frac{d_1}{h} = 0.54\left(\frac{d_c}{h}\right)^{1.275}$$

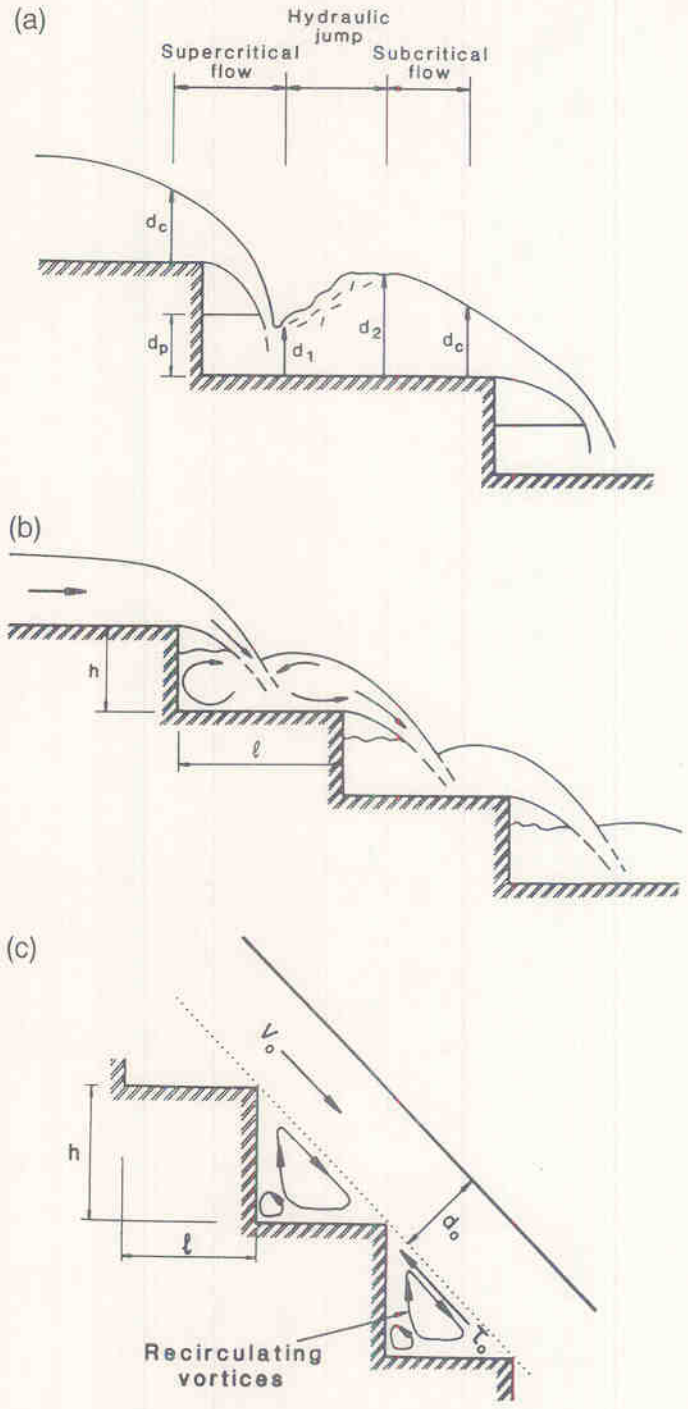

FIG. 1. (*a*) Nappe flow with fully developed hydraulic jump; (*b*) nappe flow with partially developed hydraulic jump; (*c*) skimming flow above a stepped spillway.

$$[7] \quad \frac{d_2}{h} = 1.66\left(\frac{d_c}{h}\right)^{0.81}$$

$$[8] \quad \frac{d_p}{h} = \left(\frac{d_c}{h}\right)^{0.66}$$

where d_p is the height of water in the pool behind the overfalling jet (Fig. 1*a*).

Along a stepped spillway, critical flow conditions occur near the end of each step, and [2]–[8] provide the main flow parameters for a nappe flow regime with fully developed

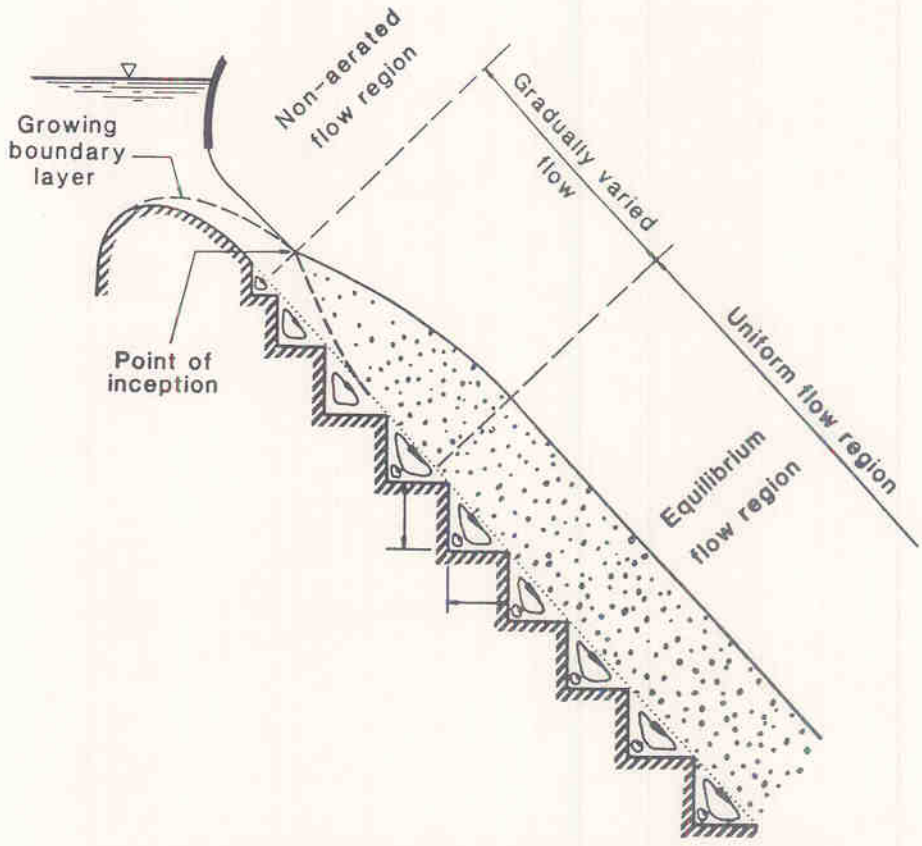

FIG. 2. Flow regions above a long stepped spillway.

hydraulic jump (Fig. 1*a*). Peyras *et al.* (1991, 1992) indicated that these equations can also be applied with reasonable accuracy to nappe flows with partially developed jump.

Energy dissipation

In a nappe flow situation with fully developed hydraulic jump, the head loss at any intermediary step equals the step height. The total head loss along the spillway, ΔH, equals the difference between the maximum head available, H_{max}, and the residual head at the bottom of the spillway, H_1, ([3]) and can be written in dimensionless form:

$$[9] \qquad \frac{\Delta H}{H_{max}} = 1 - \left[\frac{d_1}{d_c} + \frac{1}{2}\left(\frac{d_c}{d_1}\right)^2\right] \Big/ \left[\frac{3}{2} + \frac{H_{dam}}{d_c}\right]$$

where H_{dam} is the dam height and d_1 is given by [2] and [6] (Fig. 1*a*). The maximum head available and the dam height are related by $H_{max} = H_{dam} + 1.5d_c$. The residual energy is dissipated at the toe of the spillway by hydraulic jump in the dissipation basin. Combining [6] and [9], the total energy loss becomes

$$[10] \qquad \frac{\Delta H}{H_{max}} = 1 - \frac{0.54\left(\frac{d_c}{h}\right)^{0.275} + \frac{3.43}{2}\left(\frac{d_c}{h}\right)^{-0.55}}{\frac{3}{2} + \frac{H_{dam}}{d_c}}$$

In Fig. 3 the head loss ([10]) is plotted as a function of the critical flow depth and the number of steps, and compared with the experimental data (Moore 1943; Rand 1955; Stephenson 1979*a*). Figure 3 indicates that most of the flow energy is dissipated on the stepped spillway for large dams (i.e., large number of steps). Further, [10] shows good agreement with the data for a single-step structure.

Equations [9] and [10] were obtained for nappe flows with fully developed hydraulic jumps. Peyras *et al.* (1991) performed experiments for nappe flows with fully and partially developed hydraulic jumps. The rate of energy dissipation of nappe flows with partially developed hydraulic jumps was within 10% of the values obtained for nappe flows with fully developed hydraulic jumps for similar flow conditions. Therefore, it is believed that [10] may be applied to most of the nappe flow situations with reasonable accuracy.

Conditions for nappe flow regime

A number of dams have been built in South Africa with stepped spillways. From this experience, Stephenson (1991) suggested that the most suitable conditions for nappe flow situations are

$$[11a] \qquad \tan \alpha = \frac{h}{l} < 0.20$$

and

$$[11b] \qquad \frac{d_c}{h} < \frac{1}{3}$$

Skimming flow

In the skimming flow regime, the external edges of the steps form a pseudo-bottom over which the flows pass. Beneath this, horizontal axis vortices develop, filling the zone between the main flow and the step. These vortices are maintained through the transmission of shear stress from the fluid flowing past the edges of the steps (Fig. 1*c*). In

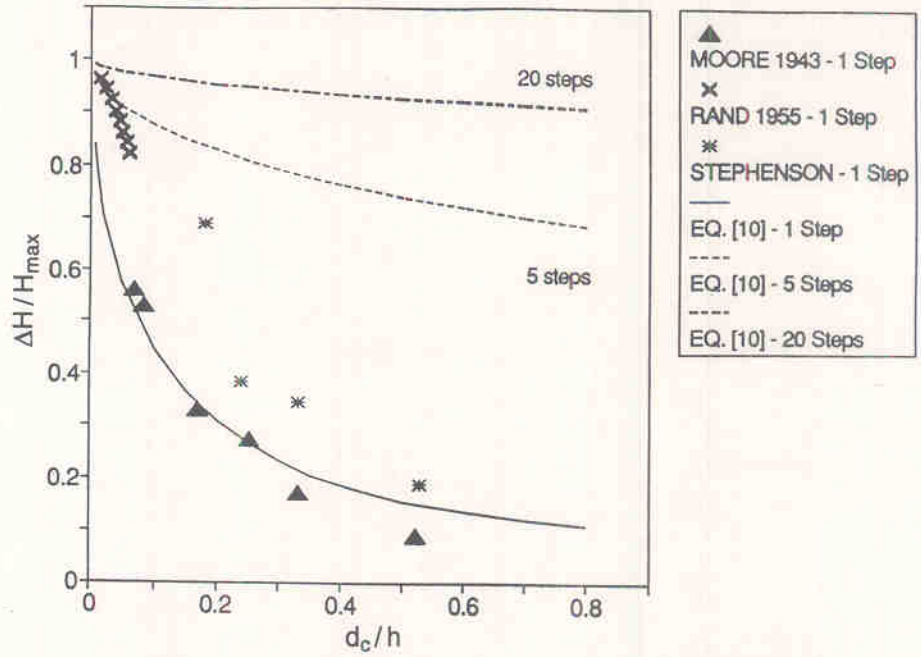

FIG. 3. Energy dissipation in nappe flow regime as a function of the number of steps. Comparison between eq. [10] and the data of Moore (1943), Rand (1955), and Stephenson (1979*a*).

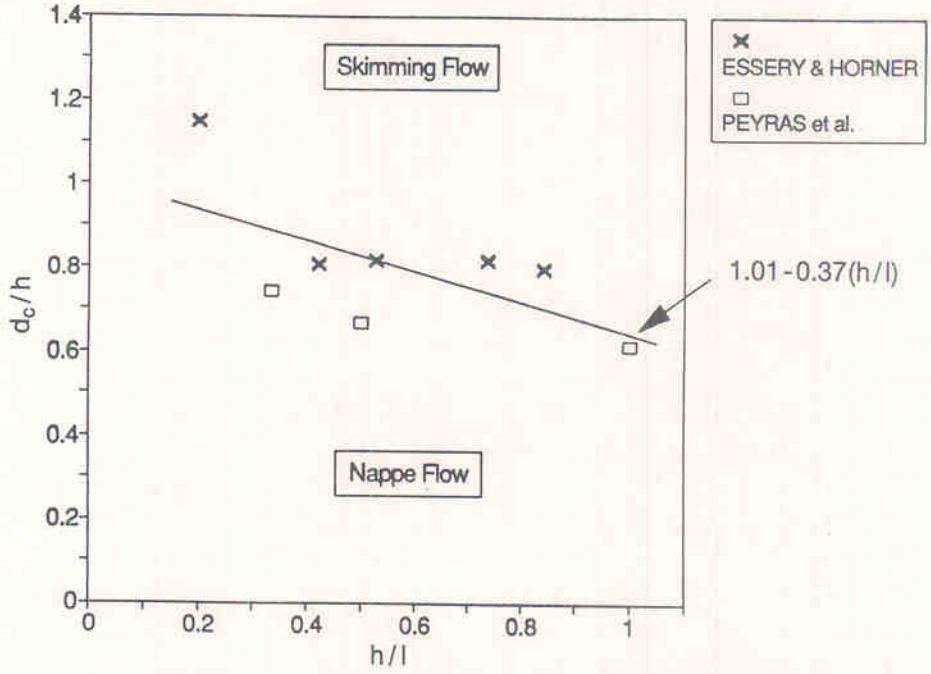

FIG. 4. Onset of skimming flow: Essery and Horner (1978) and Peyras *et al.* (1991).

addition, small-scale vorticity will be generated continuously at the corner of the steps.

Onset of skimming flow

For horizontal steps, the onset of skimming flow is a function of the discharge (i.e., critical depth) and the step height and length. Experimental data obtained by Essery and Horner (1978) and Peyras *et al.* (1991) showed that the onset flow conditions may be estimated as (Fig. 4)

$$[12] \quad \left(\frac{d_c}{h}\right)_{onset} = 1.01 - 0.37\frac{h}{l}$$

and skimming flows occur for $d_c/h > (d_c/h)_{onset}$.

It must be noted that the data of Peyras *et al.* (1991) were obtained on a gabion-stepped spillway model. The infiltration through the gabion is likely to affect the flow conditions and may explain smaller values of $(d_c/h)_{onset}$ than for Sorensen's (1985) data.

Uniform flow conditions

Assuming a long stepped spillway and that the uniform flow conditions are reached before the end of the spillway, the uniform flow depth can be deduced from the momentum equation:

$$[13] \quad \tau_0 P_w = \rho_w g A \sin \alpha$$

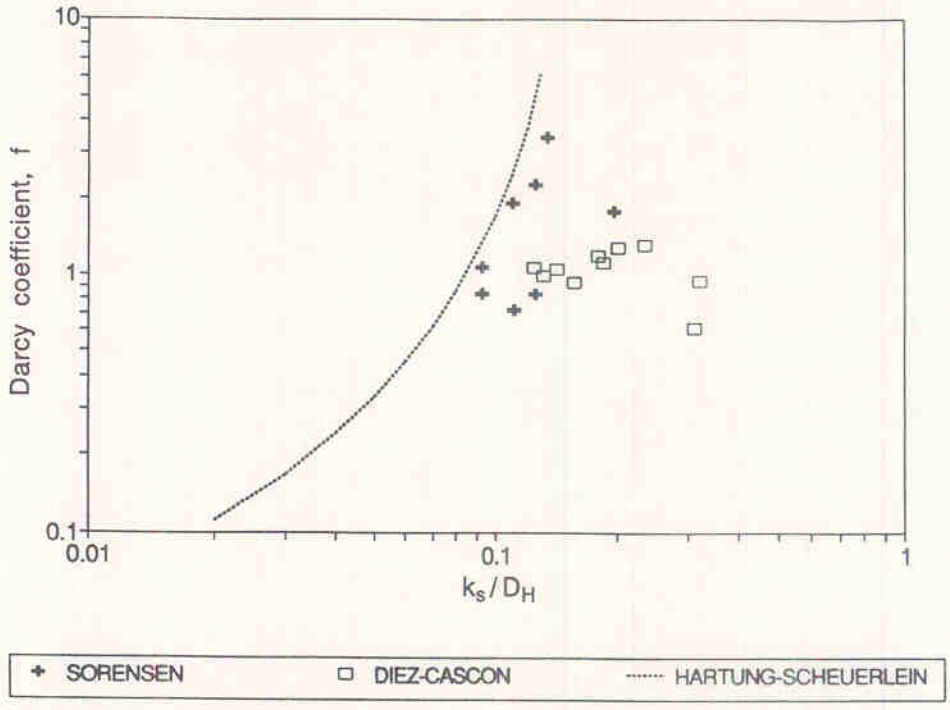

FIG. 5. Non-aerated friction factor on stepped spillways: Sorensen (1985), Diez-Cascon *et al.* (1991), Hartung and Scheuerlein (1970) for a slope, α, of 30°.

where P_w is the wetted perimeter, ρ_w the water density, g the gravity constant, A the channel cross section, and τ_0 the average shear stress between the skimming flow and the recirculating fluid underneath. The average bottom shear stress, τ_0, is defined as for an open channel flow (Henderson 1966; Streeter and Wylie 1981):

$$[14] \quad \tau_0 = \frac{f}{8}\rho_w V_0$$

where f is the Darcy coefficient (or friction factor) and V_0 the uniform non-aerated flow velocity. For a wide channel, the uniform flow parameters, V_0 and d_0, are deduced from the continuity and momentum equations, and can be written in dimensionless form:

$$[15] \quad \frac{V_0}{V_c} = \sqrt[3]{\frac{8 \sin \alpha}{f}}$$

$$[16] \quad \frac{d_0}{d_c} = \sqrt[3]{\frac{f}{8 \sin \alpha}}$$

where V_c is the critical velocity. It must be emphasized that these results were obtained for non-aerated flows. The effects of air entrainment on the flow properties are discussed in the next paragraph.

Morris (1955) and Knight and MacDonald (1979) analyzed "quasi-smooth flows" (i.e., skimming flows) over large roughness elements of rectangular cross section. Their results indicated that the classical flow resistance calculations must be modified to take into account the shape of the roughness element. The shear stress, τ_0, indicated in Fig. 1*c* and used in [13], represents the turbulent shear stress between the main stream and the recirculating fluid trapped between the steps of the spillway. For a stepped spillway, the steps form the dominant surface roughness (Sorensen 1985). If the roughness height, k_s, is estimated as the depth of a step normal to the flow (i.e., $k_s = h \cos \alpha$), the dimensions of the step are defined completely by k_s and the spillway slope. Dimensional analysis suggests that the friction factor is a function of a Reynolds number, the roughness height (k_s), and the spillway slope:

$$[17] \quad f = f_1\left(\text{Re}; \frac{k_s}{D_H}; \alpha\right)$$

where Re is the Reynolds number defined as $\text{Re} = \rho_w(V_0 D_H/\mu_w)$; D_H is the hydraulic diameter, $D_H = 4A/P_w$; and μ_w is the dynamic viscosity of water. If the uniform flow conditions are known, the Darcy coefficient can be deduced from the momentum equation ([13]):

$$[18] \quad f = \frac{8g(\sin \alpha)d_0^2}{q_w^2}\left(\frac{D_H}{4}\right)$$

where q_w is the discharge per unit width. Sorensen (1985) and Diez-Cascon *et al.* (1991) measured flow depths at the bottom of long stepped spillway models. Their data were reanalyzed using [18] and neglecting the aeration of the flow. The results are presented in Fig. 5, with the friction factor plotted as a function of the relative roughness. Figure 5 indicates friction factors in the range of 0.6–3.5, with an average value of 1.30. Such large values of the friction factor imply smaller flow velocity and greater flow depth than on a smooth spillway, and enhance the energy dissipation.

Hartung and Scheuerlein (1970) studied open channel flows on rockfill dams, with great natural roughness and steep slopes (Table 1). For slopes in the range 6–34°, and in the absence of air entrainment, their results are presented as

$$[19] \quad \frac{1}{\sqrt{f}} = -3.2 \log_{10}\left[(1.7 + 8.1 \sin \alpha)\frac{k_s}{D_H}\right]$$

TABLE 1. Experiments on stepped spillways and rockfill bottom channels

Reference	Slope (deg)	h^* (m)	q_w^* (m^2/s)	Re	k_s/D_H†	Remarks
Stepped spillways						
Moore (1943)	—	0.152, 0.457	0.017–0.186			Drop structure; one step; W = 0.279 m
Rand (1955)	—	0.198	0.25×10^{-3}–4.1×10^{-3}			Drop structure; one step; W = 0.5 m
Essery and Horner (1978)	11.3–40.1	0.03–0.05				Stepped spillway (30 steps)
Stephenson (1979*a*)	18.4–45.0	0.10, 0.15				Gabion-stepped spillway (1, 2, 3, and 4 steps)
Sorensen (1985)	52.0	0.061	0.005–0.235			Stepped spillway model (scale 1/10); 7 steps
Sorensen (1985)	52.0	0.024	0.006–0.111	6.5×10^4–3.3×10^5	0.092–0.199	Stepped spillway model (scale 1/25); 59 steps
Diez-Cascon *et al.* (1991)	53.1	0.06	0.025–0.200	1.6×10^5–6.5	0.125–0.323	Stepped spillway model (scale 1/10); H_{dam} = 3.8 m; W = 0.8 m
Peyras *et al.* (1991, 1992)	18.4–45.0	0.20	0.045–0.268			Gabion-stepped spillway model (scale 1/5); 5 steps
Stephenson (1991)	54.5					Stepped spillway, Kennedy's vale model
Rockfill bottom channels						
Hartung and Scheuerlein (1970)	6.0–34.0			8.5×10^4–2×10^6	0.02–0.2	Flow on rockfill bottom channel

*Model dimensions.
†On stepped spillway, $k_s = h\cos\alpha$.

For a slope of 30° and $k_s/D_H = 0.1$, [19] provides a value of the friction factor $f = 1.7$ of similar order of magnitude as the results obtained on stepped spillways (Fig. 5).

Energy dissipation

In skimming flow, most of the energy is dissipated in the maintenance of stable depression vortices. If uniform flow conditions are reached at the downstream end of the spillway, the total head loss is

$$[20] \quad \frac{\Delta H}{H_{max}} = 1 - \frac{\frac{d_0}{d_c}\cos\alpha + \frac{E}{2}\left(\frac{d_c}{d_0}\right)^2}{\frac{H_{dam}}{d_c} + \frac{3}{2}}$$

where E is the kinetic energy correction coefficient. Using [16], the head loss may be rewritten in terms of the friction factor, the spillway slope, the critical depth, and the dam height:

$$[21] \quad \frac{\Delta H}{H_{max}} = 1 - \left[\left(\frac{f}{8\sin\alpha}\right)^{1/3}\cos\alpha + \frac{E}{2}\left(\frac{f}{8\sin\alpha}\right)^{-2/3}\right] \Big/ \left[\frac{H_{dam}}{d_c} + \frac{3}{2}\right]$$

Equation [21] was computed for a slope (α = 52°) close to the geometry used by Sorensen (1985) and Diez-Cascon *et al.* (1991), and using two values of the friction factor, $f = 0.03$ and $f = 1.30$, that represent average flow resistance on smooth spillways and stepped spillways. The results are plotted in Fig. 6 for a uniform velocity distribution (i.e., $E = 1$), and compared with the data of Sorensen (1985), Diez-Cascon *et al.* (1991), and Stephenson (1991). Figure 6 indicates a good agreement between the experimental data and [21] computed with a friction factor $f = 1.30$ and α = 52°. Further, a comparison between the energy dissipation on smooth and stepped spillway shows a larger energy dissipation occurring on stepped spillways.

For a high dam, the residual energy term is small and [21] is similar to the expression obtained by Stephenson (1991):

$$[22] \quad \frac{\Delta H}{H_{max}} = 1 - \left[\left(\frac{f}{8\sin\alpha}\right)^{1/3}\cos\alpha + \frac{E}{2}\left(\frac{f}{8\sin\alpha}\right)^{-2/3}\right]\frac{d_c}{H_{dam}}$$

Equation [22] shows that the energy loss ratio increases with the height of the dam. For high dams, it becomes more appropriate to talk of residual head, H_{res}, than total head loss:

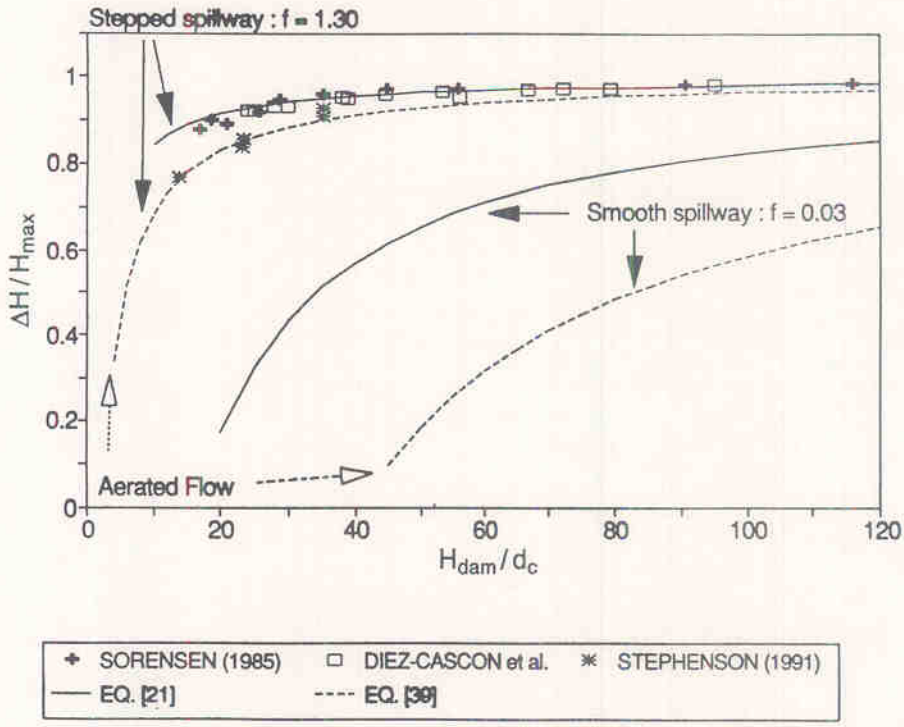

FIG. 6. Energy dissipation in skimming flow regime. Comparison between eqs. [21] and [39] and the data of Sorensen (1985), Diez-Cascon *et al.* (1991), and Stephenson (1991).

$$[23] \quad \frac{H_{res}}{d_c} = \left(\frac{f}{8 \sin \alpha}\right)^{1/3} \cos \alpha + \frac{E}{2}\left(\frac{f}{8 \sin \alpha}\right)^{-2/3}$$

Equations [21] and [23] suggest that the total energy dissipation above the spillway and the residual energy at the bottom of the spillway are functions of the friction factor, spillway slope, discharge (i.e., critical depth), and dam height. These calculations ([21] and [23]) depend critically upon the estimation of the friction factor. Figure 5 shows a large scatter of friction factor values observed on models. Further, it will be subsequently shown that the friction factor is affected significantly by the rate of aeration. Therefore [21] and [23] must be used with caution.

Notes on gabion-stepped spillways

Gabions are extensively used for earth retaining structures and for hydraulic structures (e.g., weirs, channel linings). Their advantages are (*i*) their stability, (*ii*) their low cost, and (*iii*) that they are flexible and porous (Stephenson 1979*a*, 1979*b*).

The design of gabion structures is limited by the stability of the gabions. This imposes limitations on the flow rate and flow velocity that can be accommodated. When gabions are laid parallel to the slope, there are risks of sliding or overturning failure. Stability problems may occur for discharges larger than 1 m^2/s (Peyras *et al.* 1991, 1992). Gabion-stepped spillways are more stable. Stephenson (1991) suggested that stability problems will occur for flow velocities higher than approximately 4 m/s. Peyras *et al.* (1991, 1992) indicated that gabion-stepped spillways are appropriate for discharges per unit width up to 3 m^2/s (i.e., d_c = 0.97 m). For discharges larger than 1.5 m^2/s, however, gabion wires must be reinforced or the steps must be protected by concrete caps. Inclined gabion-stepped spillways can also be used. Larger energy dissipation is observed, but their construction requires greater care.

Effects of air entrainment on stepped spillway flows

Introduction

The flow aeration, also called self-aeration,[1] was initially studied because of the effects of entrained air on the thickness of the flow. Air entrainment increases the bulk flow depth, and this is used as a design parameter for the height of spillway sidewalls (Falvey 1980). Also, the presence of air within the boundary layer reduces the shear stress between the flow layers and hence the shear force. The resulting drag reduction reduces the energy dissipation above the spillway and hence its efficiency. Further, the presence of air within high-velocity flows may prevent or reduce the damage caused by cavitation (May 1987). Recently, air entrainment on spillways and chutes has been recognized also for its contribution to the air–water transfer of atmospheric gases such as oxygen and nitrogen (Wilhelms and Gulliver 1989). This process must be taken into account for the re-oxygenation of polluted streams and rivers, and also to explain the high fish mortality downstream of large hydraulic structures.

In nappe flows, air entrainment occurs near the impact of the falling jet with the horizontal step and at the hydraulic jump. Large de-aeration also occurs downstream of the impact of the falling jet and downstream of the jump. Altogether, the net flow aeration is small, and it is believed that the effect of air entrainment on nappe flows can be neglected. This section of the paper presents an analysis of the effect of air entrainment on skimming flows. Although the flow conditions are different between a smooth and a stepped spillway, it is believed that the mechanisms of air entrainment are similar. Once the flow becomes fully developed, the stepped spillway behaves in the same way as a smooth one.

[1]Natural aeration occurring at the free surface of high velocity flows is referred to as free surface aeration or self-aeration.

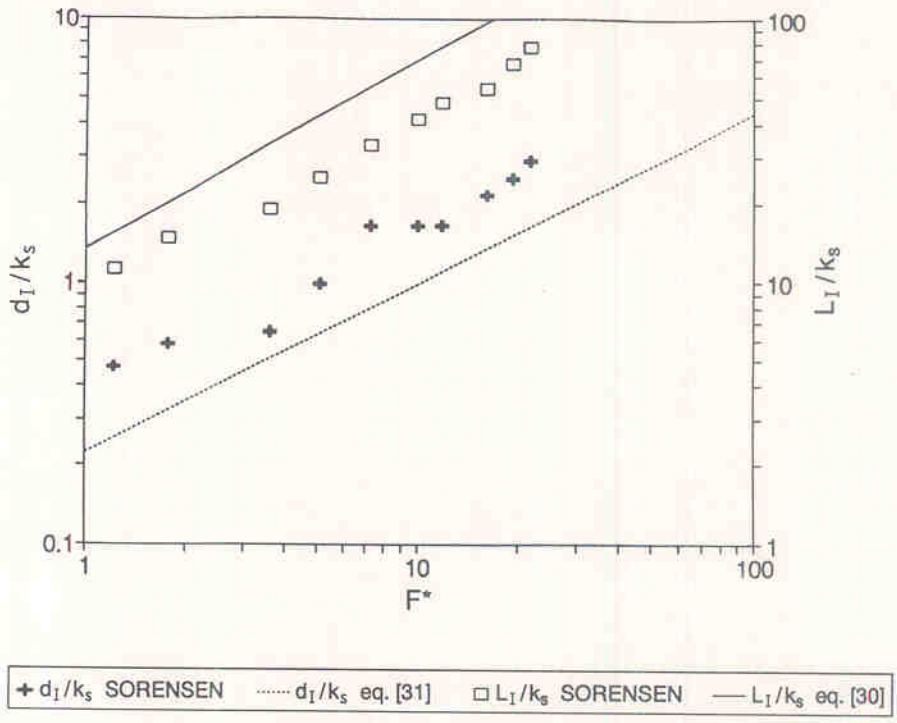

FIG. 7. Characteristics of the point of inception: Sorensen (1985).

Mechanisms of air entrainment

Air entrainment is caused by turbulent velocities acting at the air–water free surface. Through this interface, air is continuously trapped and released. Air entrainment occurs when the turbulent kinetic energy is large enough to overcome both surface tension and gravity effects. The turbulent velocity normal to the free surface, v', must overcome the surface tension pressure (Ervine and Falvey 1987) and be greater than the bubble rise velocity component for the bubbles to be carried away. These conditions are

$$[24] \quad v' > \sqrt{\frac{8\sigma}{\rho_w d_{ab}}}$$

and

$$[25] \quad v' > u_r \cos \alpha$$

where σ is the surface tension, d_{ab} the air bubble diameter, and u_r the bubble rise velocity. For bubble sizes in the range 1–100 mm, calculations using [24] and [25] suggest that air entrainment occurs for turbulent velocities, v', greater than 0.1–0.3 m/s (Chanson 1992). The flow conditions above a stepped spillway are characterized by a high degree of turbulence, and both velocity conditions are satisfied. As a consequence, large quantities of air are entrained along a stepped spillway.

For stepped spillway flows (Fig. 2), the entraining region follows a region where the flow over the spillway is smooth and glassy. Next to the boundary, however, turbulence is generated and the boundary layer grows until the outer edge of the boundary layer reaches the free surface. When the outer edge of the boundary layer reaches the free surface, the turbulence may initiate natural free surface aeration. The location of the start of air entrainment is called the point of inception. Downstream of the point of inception, a layer containing a mixture of both air and water extends gradually through the fluid. Far downstream, the flow becomes uniform, and for a given discharge, the flow depth and the air concentration and velocity distributions do not vary along the chute. This region is defined as the uniform equilibrium flow region.

Definitions

The local air concentration, C, is defined as the volume of air per unit volume. The characteristic water flow depth, d, is defined as

$$[26] \quad d = \int_0^{Y_{90}} (1 - C)\, dy$$

where y is measured perpendicular to the spillway surface and Y_{90} is the depth where the local air concentration is 90%. The depth-averaged mean air concentration, C_{mean}, is defined as

$$[27] \quad (1 - C_{mean}) Y_{90} = d$$

The average water velocity, U_w, is defined as

$$[28] \quad U_w = \frac{q_w}{d}$$

Point of inception

On smooth spillways, the position of the point of inception is primarily a function of the discharge and the spillway roughness. Keller and Rastogi (1977) suggested the following:

$$[29a] \quad \frac{L_I}{k_s} = f_2(F^*; \sin \alpha)$$

$$[29b] \quad \frac{d_I}{k_s} = f_3(F^*; \sin \alpha)$$

where L_I is the distance from the start of growth of the boundary layer to the point of inception; d_I is the depth at

TABLE 2. Flow conditions for Straub and Anderson's (1958), Aivazyan's (1986), and Jevdjevich and Levin's (1953) data

Experiment	Slope (deg)	k_s (mm)	k_s/D_H	Re	C_e	Comments
St. Anthony Falls*	7.5–75	0.71	0.003–0.016	4.7×10^5–2×10^6	0.15–0.73	Spillway model (W = 0.457 m); artificial roughness
Aivazyan†	14–31	0.1–10	0.005–0.04	1.7×10^5–2.8×10^7	0.21–0.54	Prototype and large spillway model (W = 0.25 to 6 m); planed boards, wood, rough concrete, and rough stone masonry
Mostarsko Blato‡	—	10–20	0.015–0.035	8.3×10^4–3×10^7	0.58–0.66	Prototype; wide channel (W = 5.75 m); stone lining

*Straub and Anderson (1958).
†Aivazyan (1986).
‡Jevdjevich and Levin (1953).

TABLE 3. Average air concentration in uniform self-aerated flows

Slope (deg)	C_e*	Y_{90}/d_e*	f_e/f†
7.5	0.1608	1.192	0.968
15.0	0.2411	1.318	0.871
22.5	0.3100	1.449	0.765
30.0	0.4104	1.696	0.614
37.5	0.5693	2.322	0.389
45.0	0.6222	2.647	0.313
60.0	0.6799	3.124	0.228
75.0	0.7209	3.583	0.168
0.0	0.000	1.000	1.000

*Data from Straub and Anderson (1958).
†Computed from eq. [36].

the point of inception measured normal to the free surface; and F^* is a Froude number defined in terms of the roughness height, $F^* = q_w/\sqrt{g(\sin\alpha)k_s^3}$. For smooth concrete spillways, Wood (1983) estimated [29] as

$$[30]\quad \frac{L_I}{k_s} = 13.6(\sin\alpha)^{0.0796}(F^*)^{0.713}$$

$$[31]\quad \frac{d_I}{k_s} = \frac{0.223}{(\sin\alpha)^{0.04}}(F^*)^{0.643}$$

On stepped spillways, the position of the start of air entrainment is a function of the discharge, spillway roughness, step geometry, and spillway geometry. Sorensen (1985) recorded the position of the start of air entrainment and the flow depth at the nearest measurement station. His results are presented as L_I/k_s and d_I/k_s versus the Froude number, F^*, as shown in Fig. 7. Sorensen's (1985) results are also compared with [30] and [31], where the roughness, k_s, was estimated as the depth of a step normal to the free surface (i.e., $k_s = h\cos\alpha$). Figure 7 shows that [30] overestimates the location of the point of inception by approximately 40%. This result indicates that the growth of the boundary layer is enhanced by the geometry of the steps.

Uniform flow region

Average air concentration

On stepped spillways, a large quantity of air is entrained along the channel, and the amount of air entrained is usually defined in terms of the average air concentration.[2] The analysis of self-aerated flow measurements on smooth spillways (Table 2) (Straub and Anderson 1958; Aivazyan 1986) showed that the average air concentration for uniform flow conditions, C_e, is independent of the upstream geometry and flow conditions (i.e., discharge, flow depth, roughness) and is a function of the slope only (Wood 1983; Chanson 1992). Figure 8 shows the average air concentration, C_e, as a function of the slope, α, for Straub and Anderson's (1958) data obtained on a model and the field data presented by Aivazyan (1986). For slopes flatter than 50°, the average air concentration may be estimated as

$$[32]\quad C_e = 0.9\sin\alpha$$

Using the data of Hartung and Scheuerlein (1970) obtained with great natural roughness and steep slopes (Table 1), Knauss (1979) indicated that the quantity of air entrained was estimated as

$$[33]\quad C_e = 1.44(\sin\alpha) - 0.08$$

This result is of similar form as [32]. Figure 8 compares [32] and [33] with experimental data. These results show a comparable rate of air entrainment for both smooth and rough flows. On stepped spillways, the uniform air concentration is expected to be siimlar to the results obtained on a smooth spillway, where the mean air concentration is a function of the slope only (Table 3).

Friction factor

For uniform aerated flows the momentum equation yields

$$[34]\quad f_e = \frac{8g(\sin\alpha)d_e^2}{q_w^2}\left(\frac{D_H}{4}\right)$$

where f_e is the friction factor for the uniform air–water mixture and d_e is the water flow depth (i.e., [26]) in uniform equilibrium flow. If f is the friction factor of non-aerated flow, dimensional analysis suggests that the ratio f_e/f is a function of the average air concentration, the Reynolds number, and the relative roughness:

[2]The quantity of air entrained within the flow is related to the mean air concentration by $q_{air}/q_w = C_{mean}/(1 - C_{mean})$.

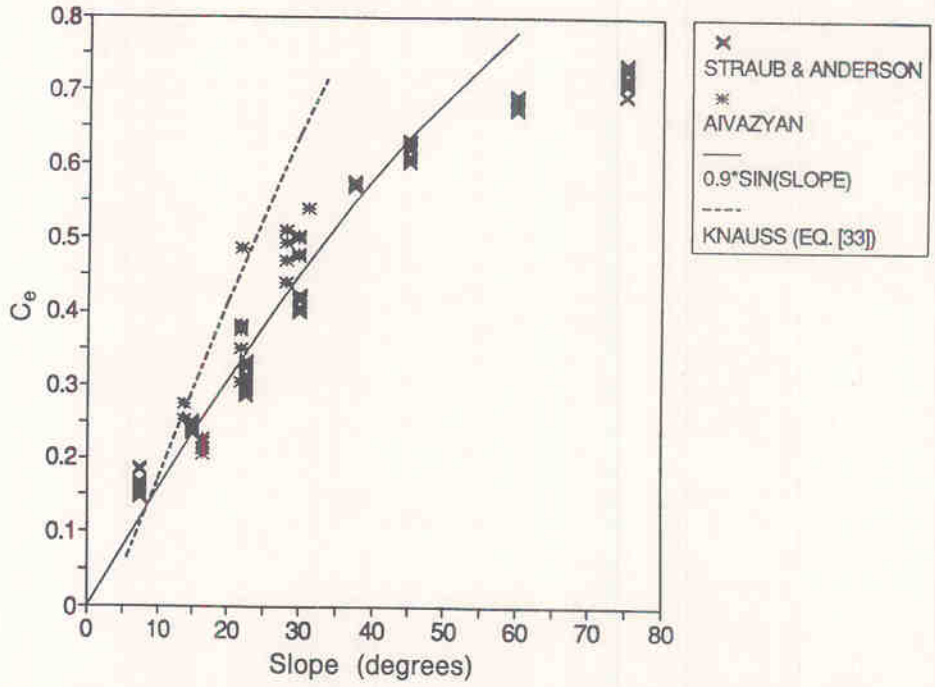

FIG. 8. Uniform equilibrium air concentration, C_e, as a function of the spillway slope: Straub and Anderson (1958), Aivazyan (1986), and Knauss (1979).

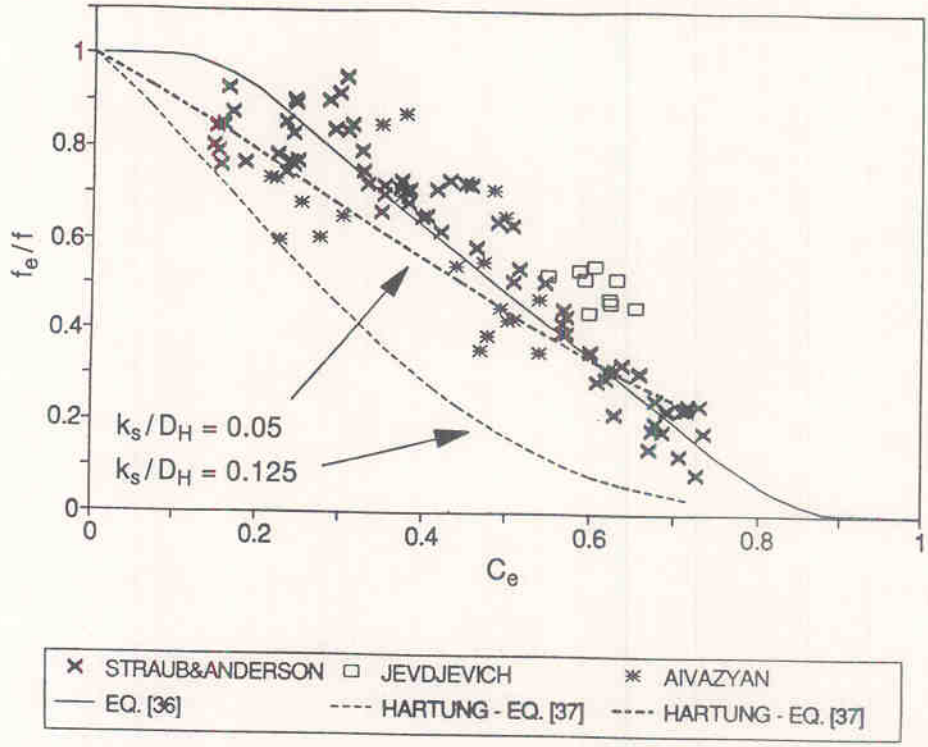

FIG. 9. Relative friction factor, f_e/f, as a function of the uniform air concentration, C_e, on smooth spillways (Straub and Anderson (1958), Jevdjevich and Levin (1953), and Aivazyan (1986)) and rockfill channels (Hartung and Scheuerlein (1970)).

[35] $$\frac{f_e}{f} = f_4\left(C_e;\ \mathrm{Re};\ \frac{k_s}{D_H}\right)$$

In uniform self-aerated flows for a smooth channel, the data of Jevdjevich and Levin (1953), Straub and Anderson (1958), and Aivazyan (1986) were analyzed using [34]. The results are presented in Fig. 9, where the ratio f_e/f is plotted as a function of the average air concentration, f being calculated using the Colebrook–White formula. For these data, the effect of the Reynolds number and the relative roughness on the ratio f_e/f is small, and [35] is estimated as

[36] $$\frac{f_e}{f} = 0.5\left\{1 + \tanh\left[0.70\frac{0.490 - C_e}{C_e(1 - C_e)}\right]\right\}$$

where $\tanh(x) = [\exp(x) - \exp(-x)]/[\exp(x) + \exp(-x)]$. A general trend is that, for a given non-aerated friction factor, the friction factor for aerated flow, f_e, decreases when the average air concentration increases.

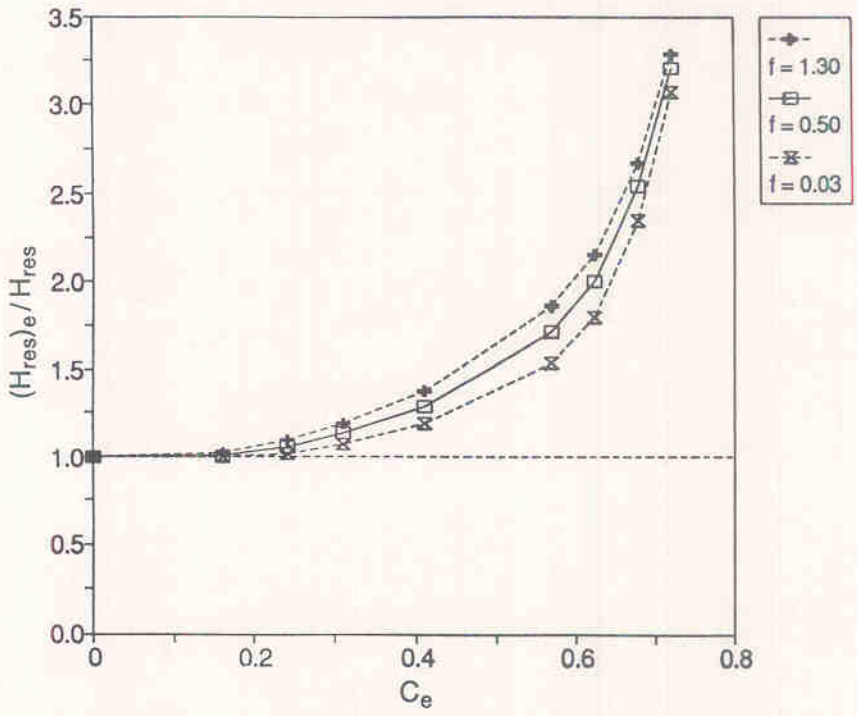

FIG. 10. Effects of air entrainment and spillway slope on the residual energy, eq. [41].

Further, Hartung and Scheuerlein (1970) studied open channel flows on rockfill dams. The extremely rough bottom induced a highly turbulent flow with air entrainment. In the presence of air entrainment, their results are presented as

$$[37] \quad \frac{f_e}{f} = \frac{1}{[1 - 3.2\sqrt{f}\log_{10}(1 - C_e)]^2}$$

where C_e is estimated from [33] and f is the non-aerated friction factor estimated by [19]. Their results also show a reduction in the ratio f_e/f with an increase in air concentration (Fig. 9). Also, in fully rough turbulent flows, [37] suggests that the ratio f_e/f decreases with increasing roughness.

Figure 9 indicates a similar trend on both smooth and extremely rough channels; that is, a substantial drag reduction when the air concentration increases above 10–20% (i.e., $\alpha > 10°$). It is believed that the same mechanisms of drag reduction apply also to stepped spillways, and that [36] and [37] can be used to provide a first estimate of the relative friction factor of aerated flows on stepped spillways.

Uniform flow parameters on stepped spillways

In uniform self-aerated flows, the flow parameters and energy dissipation can be deduced from the chute geometry (i.e., slope, roughness, width) and from the discharge. For any slope α, the average air concentration for uniform flow, C_e, can be obtained from Fig. 8. If the value of the friction factor for non-aerated flows, f, is available, Fig. 9 can be used to provide the friction factor for an aerated flow, f_e, as a function of the mean air concentration, C_e. The characteristic depth, d_e, may be deduced from [34]. For a wide channel (i.e., $D_H \sim 4d_e$), [34] yields

$$[38] \quad d_e = \left(\frac{q_w^2 f_e}{8g \sin \alpha}\right)^{1/3}$$

Knowledge of the equilibrium air concentration, C_e, friction factor, f_e, and flow depth, d_e, provides the characteristic depth, Y_{90} (Table 3): $Y_{90} = d_e/(1 - C_e)$. The depth Y_{90} takes into account the bulk of the flow and may be used as a design parameter for the height of sidewalls.

Energy dissipation

If the flow is uniform at the downstream end of the spillway, the energy dissipation along the stepped spillway with aerated flow, ΔH_e, is

$$[39] \quad \frac{\Delta H_e}{H_{max}} = 1 - \left[\left(\frac{f_e}{8 \sin \alpha}\right)^{1/3} (\cos \alpha) + \frac{E}{2}\left(\frac{f_e}{8 \sin \alpha}\right)^{-2/3}\right] \Big/ \left[\frac{H_{dam}}{d_c} + \frac{3}{2}\right]$$

Equation [39] differs from [21] by using the friction factor for aerated flow. Equation [39] was computed for a slope, α, of 52° and two values of non-aerated friction factor, f = 0.03 and 1.30. In Fig. 6, the results are compared with non-aerated flow calculations ([21]) and the data of Sorensen (1985), Diez-Cascon *et al.* (1991), and Stephenson (1991), neglecting the effects of air entrainment. It must be emphasized that the measurements of Sorensen (1985), Diez-Cascon *et al.* (1991), and Stephenson (1991) took into account the flow bulking due to air entrainment, and that the measured flow depths were not the uniform flow depth, d_e. Therefore the friction factor values and energy dissipation computed from their data ([18] and [20]) are overestimated and differ from [34] and [39].

Figure 6 shows that the rate of energy dissipation on smooth spillways is affected much more by air entrainment than on stepped spillways. As the mean air concentration increases with the slope and the friction factor decreases with the mean air concentration, the effects of air entrainment are more significant on steep slopes. On stepped spillways, air entrainment seems to have little effect on the energy

TABLE 4. Energy dissipation on stepped spillways

	$\Delta H/H_{max}$							
			Skimming flow†					
	Nappe flow*		α = 30°		α = 45°		α = 60°	
H_{dam}/d_c	d_c/h = 0.1, eq. [10]	d_c/h = 0.6, eq. [10]	Unaerated eq. [21]	Aerated eq. [39]	Unaerated eq. [21]	Aerated eq. [39]	Unaerated eq. [21]	Aerated eq. [39]
10	0.446	0.762	0.856	0.828	0.846	0.723	0.842	0.629
20	0.704	0.873	0.923	0.908	0.918	0.852	0.916	0.802
30	0.798	0.913	0.948	0.937	0.944	0.899	0.942	0.865
40	0.846	0.934	0.960	0.952	0.957	0.823	0.956	0.897
50	0.876	0.947	0.968	0.962	0.966	0.938	0.965	0.917
60	0.896	0.955	0.973	0.968	0.971	0.948	0.971	0.931
70	0.911	0.962	0.977	0.972	0.975	0.955	0.975	0.940
80	0.922	0.966	0.980	0.976	0.978	0.961	0.978	0.948
90	0.930	0.980	0.982	0.978	0.981	0.965	0.980	0.953
100	0.937	0.973	0.984	0.981	0.983	0.969	0.982	0.958
120	0.948	0.977	0.986	0.984	0.985	0.974	0.985	0.965
150	0.958	0.982	0.989	0.987	0.988	0.979	0.988	0.972
200	0.968	0.986	0.992	0.990	0.991	0.984	0.991	0.979

*The number of steps equals H_{dam}/h and is given by $(H_{dam}/d_c) \times (d_c/h)$.
†Calculations made assuming f = 1.30.

dissipation. But it is more appropriate to consider the residual energy. For aerated flows, the residual energy at the bottom of the spillway $(H_{res})_e$ is

$$[40] \quad \frac{(H_{res})_e}{d_c} = \left(\frac{f_e}{8 \sin \alpha}\right)^{1/3} (\cos \alpha) + \frac{E}{2}\left(\frac{f_e}{8 \sin \alpha}\right)^{-2/3}$$

The relative increase in residual energy due to flow aeration is

$$[41] \quad \frac{(H_{res})_e}{H_{res}} = \left(\frac{f_e}{f}\right)^{1/3} \left[\frac{1 + 4\frac{E}{f}(\tan \alpha)\left(\frac{f}{f_e}\right)}{1 + 4\frac{E}{f} \tan \alpha}\right]$$

where H_{res} is obtained from [23] and f_e/f is estimated from [36] and [37]. The aeration of the flow decreases the friction factor and increases the kinetic energy of the flow. As a result, the residual energy increases with the air concentration. Equation [41] is plotted as a function of the mean air concentration for a smooth spillway (i.e., f = 0.03) and a stepped spillway (i.e., f = 1.30) in Fig. 10. Figure 10 shows that the residual energy is affected by the flow aeration for mean air concentrations larger than 40%. Figure 8 and Table 3 indicate that a mean air concentration of 40% is obtained for a slope, α, of 30°. Hence these results suggest that the effects of air entrainment on the residual energy cannot be neglected for slopes larger than 30°, for both smooth and stepped spillway types. Although Fig. 6 suggests that the total energy dissipation is only slightly overestimated, Fig. 10 shows that the residual energy is strongly underestimated if the effect of air entrainment is neglected.

Discussion

Table 4 presents a comparison between the energy dissipation in nappe flows ([10]) and skimming flows ([21] and [39]) for various slopes and dam heights. The results indicate that nappe flow situations do not always provide the maximum energy dissipation. If the spillway is long enough (i.e., if uniform flow conditions are obtained), and for identical flow conditions and dam height, the maximum energy dissipation along the spillway is obtained for a skimming flow regime above a relatively flat stepped spillway. On steep spillways, the flow aeration reduces the flow resistance and hence the rate of energy dissipation.

For short stepped spillways, [21] and [39] are incorrect, as uniform flow conditions do not occur. In such cases, it is believed that nappe flow situations provide the maximum energy dissipation as suggested by Ellis (1989) and Peyras *et al.* (1992).

Gradually varied flow region

On smooth spillways, a simple analysis of the continuity equation for air and the energy equation provides two simultaneous differential equations in terms of the average air concentration and the flow depth in the gradually varied flow region (Chanson 1992). These equations can be solved with explicit numerical methods to determine the air entrainment which will occur on chutes and spillways. However, predictions of self-aeration depend upon the estimation of the air bubble rise velocity, the entrainment velocity, and the friction factor. At the present time, no such experimental data is available for prototype stepped spillways. Although the air entrainment mechanisms are comparable to those observed on smooth spillways, the high level of turbulence is likely to modify the estimations of the rise velocity and entrainment velocity. Additional measurements on stepped spillways are also required to estimate the flow resistance.

Conclusion

Two types of flow regime exist above a stepped spillway: nappe flow and skimming flow. For flat slopes or low discharges, the water proceeds in a series of plunges from one step to the next in what is called nappe flow. For steep slopes and large discharges, the water flows as a coherent stream over large recirculating vortices trapped between the

steps and the main stream in a skimming flow regime. Equation [12] provides an estimate of the onset of skimming flow.

In both nappe flow and skimming flow regimes, the design of a stepped spillway is a very efficient method to dissipate a large part of the flow energy along the spillway, and up to 99% of the total head available can be dissipated (Table 4).

Flow conditions above a stepped spillway are affected by the air entrainment. A comparison between aerated skimming flows and self-aerated flows above smooth and extremely rough channels showed that the mean air concentration tends to a uniform air concentration, C_e, as a function of the slope only ([32] and [33]). Further, the presence of air reduces the friction factor in uniform aerated flows for slopes steeper than 10°. The observed drag reduction reduces the total energy dissipation above the spillway (Fig. 5) and, hence, the efficiency of a stepped spillway for slopes steeper than 30° (Fig. 10).

At the present time, there is a lack of information on the estimate of the non-aerated friction factor and on the flow properties in the gradually varied flow region (Fig. 2). Measurements of air concentration and velocity in aerated flows above stepped spillways are also required.

Aivazyan, O.M. 1986. Stabilized aeration on chutes. Gidrotekhnicheskoe Stroitel'stvo, No. 12, pp. 33–40. Also in Hydrotechnical Construction **20**: 713–722.

Chanson, H. 1992. Air entrainment in chutes and spillways. Research Report No. CE 133, Department of Civil Engineering, University of Queensland, Australia.

Degoutte, G., Peyras, L., and Royet, P. 1990. Discussion of "Skimming flow in stepped spillways." ASCE Journal of Hydraulic Engineering, **118**(1): 111–114.

Diez-Cascon, J., Blanco, J.L., Revilla, J., and Garcia, R. 1991. Studies on the hydraulic behaviour of stepped spillways. International Water Power and Dam Construction, September, pp. 22–26.

Ellis, J. 1989. Guide to analysis of open-channel spillway flow. 2nd ed. CIRIA Technical Note No. 134, Construction Industry Research and Information Association, London, United Kingdom.

Ervine, D.A., and Falvey, H.T. 1987. Behaviour of turbulent water jets in the atmosphere and in plunge pools. Proceedings of the Institution Civil Engineers, Part 2, **83**: 295–314.

Essery, I.T.S., and Horner, M.W. 1978. The hydraulic design of stepped spillways. 2nd ed. CIRIA Report No. 33, Construction Industry Research and Information Association, London, United Kingdom.

Falvey, H.T. 1980. Air–water flow in hydraulic structures. U.S. Bureau of Reclamation Engineering Monograph, No. 41, Denver, Colo.

Frizell, K.H., and Mefford, B.W. 1991. Designing spillways to prevent cavitation damage. Concrete International, May, pp. 58–64.

Hartung, F., and Scheuerlein, H. 1970. Design of overflow rockfill dams. Proceedings, 10th International Congress On Large Dams, Montréal, Que., Q. 36, R. 35, pp. 587–598.

Henderson, F.M. 1966. Open channel flow. MacMillan Company, New York, N.Y.

Jevdjevich, V., and Levin, L. 1953. Entrainment of air in flowing water and technical problems connected with it. Proceedings of the 5th International Association for Hydraulic Research Congress, Minneapolis, Minn., pp. 439–454.

Keller, R.J., and Rastogi, A.K. 1977. Design chart for predicting critical point on spillways. ASCE Journal of the Hydraulic Division, **103**(HY12): 1417–1429.

Knauss, J. 1979. Computation of maximum discharge at overflow rockfill dams (a comparison of different model test results). Proceedings, 13th International Congress On Large Dams, New Delhi, India, Q. 50, R. 9, pp. 143–159.

Knight, D.W., and MacDonald, J.A. 1979. Hydraulic resistance of artificial strip roughness. ASCE, Journal of the Hydraulics Division, **105**(HY6): 675–690.

May, R.W.P. 1987. Cavitation in hydraulic structures: occurrence and prevention. Hydraulics Research Report, No. SR 79, Wallingford, United Kingdom.

Moore, W.L. 1943. Energy loss at the base of a free overfall. ASCE Transactions, **108**: 1343–1360.

Morris, H.M. 1955. A new concept of flow in rough conduits. ASCE Transactions, **120**: 373–410.

Peterka, A.J. 1953. The effect of entrained air on cavitation pitting. Joint Meeting Paper, International Association for Hydraulic Research/American Society of Civil Engineers, Minneapolis, Minn., pp. 507–518.

Peyras, L., Royet, P., and Degoutte, G. 1991. Ecoulement et dissipation sur les déversoirs en gradins de gabions (Flows and dissipation of energy on gabion weirs). Journal La Houille Blanche, No. 1, pp. 37–47.

Peyras, L., Royet, P., and Degoutte, G. 1992. Flow and energy dissipation over stepped gabion weirs. ASCE Journal of Hydraulic Engineering, **118**(5): 707–717.

Rajaratnam, N. 1990. Skimming flow in stepped spillways. ASCE Journal of Hydraulic Engineering, **116**(4): 587–591.

Rand, W. 1955. Flow geometry at straight drop spillways. ASCE Proceedings, **81**: 1–13.

Rouse, H. 1936. Discharge characteristics of the free overfall. Civil Engineering, **6**: 257.

Russell, S.O., and Sheehan, G.J. 1974. Effect of entrained air on cavitation damaged. Canadian Journal of Civil Engineering, **1**: 97–107.

Sorensen, R.M. 1985. Stepped spillway hydraulic model investigation. ASCE Journal of Hydraulic Engineering, **111**(12): 1461–1472.

Stephenson, D. 1979*a*. Gabion energy dissipators. Proceedings, 13th International Congress On Large Dams, New Delhi, India, Q. 50, R. 3, pp. 33–43.

Stephenson, D. 1979*b*. Rockfill in hydraulic engineering. Elsevier Scientific Publishing Co., Amsterdam, The Netherlands.

Stephenson, D. 1991. Energy dissipation down stepped spillways. International Water Power and Dam Construction, September, pp. 27–30.

Straub, L.G., and Anderson, A.G. 1958. Experiments on self-aerated flow in open channels. ASCE Journal of the Hydraulics Division, **84**(HY7): 1890-1 to 1890-35.

Streeter, V.L., and Wylie, E.B. 1981. Fluid mechanics. 1st SI metric edition. McGraw-Hill, Singapore.

Vital, N., and Porey, P.D. 1987. Design of cascade stilling basins for high dam spillways. ASCE Journal of Hydraulic Engineering, **113**(2): 225–237.

White, M.P. 1943. Discussion of "Energy loss at the base of a free overfall." ASCE Transactions. **108**: 1361–1364.

Wilhelms, S.C., and Gulliver, J.S. 1989. Self-aerating spillway flow. Proceedings of the ASCE National Conference on Hydraulic Engineering, New Orleans, La., pp. 881–533.

Wood, I.R. 1983. Uniform region of self-aerated flow. **109**(3): 447–461.

Wood, I.R. 1985. Air water flows. Proceedings of the 21st International Association of Hydraulic Research Congress, Melbourne, Australia, pp. 18–29.

Wood, I.R., Ackers, P., and Loveless, J. 1983. General method for critical point on spillways. ASCE Journal of Hydraulic Engineering, **109**(2): 308–312.

List of symbols

A cross-sectional area (m^2)

C air concentration defined as the volume of air per unit volume

C_e	equilibrium depth-averaged air concentration for uniform flow
C_{mean}	depth-averaged air concentration defined as $(1 - Y_{90})C_{mean} = d$
D_H	hydraulic diameter (m) defined as $D_H = 4\frac{A}{P_w}$
d	flow depth measured normal to the channel slope at the edge of a step; characteristic depth (m) defined as $d = \int_{y=0}^{y=Y_{90}} (1 - C)\,dy$
d_I	flow depth at the inception point (m)
d_{ab}	air bubble diameter (m)
d_b	flow depth at the brink of a step (m)
d_c	critical flow depth (m)
d_e	uniform aerated flow depth (m)
d_0	uniform non-aerated flow depth (m)
d_p	flow depth in the pool beneath the nappe (m)
E	kinetic energy correction coefficient (Coriolis coefficient)
Fr	Froude number defined as $Fr = q_w/\sqrt{gd^3}$
F^*	Froude number defined as $F^* = q_w/\sqrt{g(\sin\alpha)\,k_s^3}$
f	friction factor for non-aerated flow
f_e	friction factor for aerated flow
g	gravity constant (m/s^2)
H	total head (m)
H_{dam}	dam height (m)
H_{max}	maximum head available ($= H_{dam} + \frac{3}{2}d_c$) (m)
H_{res}	residual head at the bottom of the spillway (m)
h	height of steps (m)
k_s	equivalent uniform sand roughness (m); step dimension normal to the flow ($k_s = h\cos\alpha$)
L	distance along the spillway (m)
L_I	distance from the start of growth of boundary layer to the point of inception (m)
l	horizontal length of steps (m)
P_w	wetted perimeter (m)
Q	discharge (m^3/s)
q	discharge per unit width (m^2/s)
Re	Reynolds number defined as $Re = \rho_w U_w D_H/\mu_w$
U_w	flow velocity ($= q_w/d$) (m/s)
u_r	rise bubble velocity (m/s)
V	velocity (m/s)
V_c	critical velocity (m/s)
V_0	uniform non-aerated flow velocity (m/s)
v'	root-mean-square of lateral component of turbulent velocity (m/s)
W	channel width (m)
Y_{90}	characteristic depth (m) where the air concentration is 90%
y	distance from the bottom, measured perpendicular to the spillway surface (m)
α	spillway slope
ΔH	head loss (m)
μ	dynamic viscosity ($N\cdot s/m^2$)
ρ	density (kg/m^3)
σ	surface tension between air and water (N/m)
τ_0	average bottom shear stress (Pa)

Subscript

c	critical flow conditions
e	equilibrium uniform aerated flow
0	uniform non-aerated flow
w	water flow